Imam, M. A., Froes, F. H. & Reddy R. M. (2013). *Cost-Affordable Titanium IV*. (Key Engineering Materials, 551). Switzerland: Trans Tech Publications, 161-171.
DOI: http://dx.doi.org/10.4028/www.scientific.net/KEM.551.161

Comparison of Microstructure and Properties of Ti-6Al-7Nb Alloy Processed by Different Powder Metallurgy Routes

L. Bolzoni[1,2,a], N. Hari Babu[2,b], E.M. Ruiz-Navas[1,c], E. Gordo[1,d]

[1]Department of Materials Science and Engineering, University Carlos III of Madrid,
Avda. de la Universidad, 30, 28911 Leganes, Madrid - Spain

[2]BCAST – Brunel Centre for Advanced Solidification Technology
Brunel University, Uxbridge, Middlesex, UB8 3PH, London - UK

[a]leandro.bolzoni@brunel.ac.uk, [b]mtsthbn@brunel.ac.uk, [c]emruiz@ing.uc3m.es,
[d]elena.gordo@uc3m.es

Abstract

Abstract: The Ti-6Al-7Nb alloy was specially developed to replace the well-known Ti-6Al-4V alloy in biomedical applications due to supposed cytotoxicity of vanadium in the human body. This alloy is normally fabricated by conventional ingot metallurgy by forging bulk material. Nevertheless, powder metallurgy techniques could be used to obtain this alloy with specific properties. This is because by changing the processing parameters, such as the sintering temperature, it is possible to vary the porosity level and to tailor the final properties. This work deals with the production of the Ti-6Al-7Nb alloy by means of the master alloy addition variant of the blending elemental approach. The powder is processed by means of different powder metallurgy routes considering diverse processing conditions for each method. The materials are characterised in terms of microstructural features, relative density and hardness. Homogeneous microstructures as well as properties comparable to those of the wrought alloy are generally obtained.

Keywords: Ti-6Al-7Nb, titanium powder metallurgy, blending elemental (BE), master alloy (MA) addition, homogeneous microstructure

1. Introduction

Titanium is well known to be characterised by an outstanding combination of properties such as the highest specific strength (strength to density ratio) among metals, incomparable corrosion resistance in many aggressive environment and biocompatibility. Moreover, titanium has the ability to retain its mechanical properties to relatively high service temperatures; normally up to approximately 500ºC. Nonetheless, titanium is only chosen for applications where the final cost of a product is not the main issue or it is not as important as the combination of properties that the material can provide. The main reason for the limitation of the employment of titanium at industrial level is primarily due to two factors: (1) higher extraction and (2) higher manufacturing costs in comparison to steel and aluminium. Actually, for the production of the same ingot, titanium will cost 30 times more than steel and 6 times more than aluminium [1].

The high extraction cost of elemental titanium from its ores is because of the high stability of its oxides and compounds due to the great affinity that titanium has for interstitials like for interstitials like oxygen, nitrogen, hydrogen and carbon. The amount of these elements should be kept as low as possible since very small percentages drastically lower the ductility.

The high manufacturing costs derive from both the necessity to maintain very low interstitials contents and the poor machinability of titanium caused by its relative low thermal conductivity. On the base of this scenario, titanium and its alloys have been mainly used in the aerospace and aeronautic industry, marine and chemical applications, and to fabricate biomedical devices and prostheses.

When it comes to biomedical applications, titanium is favoured by low density, superior biocompatibility and elastic modulus lower than other metallic biomaterials such as precious metals Co-Cr alloys and austenitic stainless steel. The first applications of elemental titanium as biomaterial date back to the nineteen fifties. Subsequently, the titanium workhorse Ti-6Al-4V alloy was adopted because the mainstream approach taken for the introduction of orthopaedic materials has involved adaptation of existing materials [2]. Lately, vanadium-free titanium alloys were developed due to the potential cytotoxicity and adverse reaction of vanadium with the body tissues. In many of these alloys, non-toxic but heavy alloying elements like niobium, zirconium and tantalum are specifically employed [3]. A typical example is the Ti-6Al-7Nb alloy fabricated by forging bulk material for hip prosthesis stems which was developed by Semlitsch et al. in the nineteen eighties [4].

The processing of titanium and its alloys by means of powder metallurgy techniques is claimed to be a way to reduce the production cost due to the intrinsic advantages of these near-net-shape or net-shape methods. This is because powder metallurgy techniques have a much higher yield of material and the need of machining is limited or avoided, which translate into lower losses and scraps of expensive material. A further cost reduction can be obtained by employing blending elemental (BE) powders instead of more expensive prealloyed (PA) powder because the BE approach has been identified as the cheapest way to obtained titanium alloys [5]. Moreover, the employment of nowadays available hydride-dehydride (HDH) powders eliminates the problems related with the presence of the chlorides of sponge powders. In sponge powders, the residual chlorides left from the extraction process (Kroll's process) generate porosity filled with gas during the sintering step. This porosity is very difficult to eliminate even by means of post-processing techniques such as hot isostatic pressing (HIP) and can cause explosion during the welding of the material [6].

This work focuses on the production of the Ti-6Al-7Nb alloy fabricated by means of the master alloy addition variant of the blending elemental approach using a HDH elemental titanium powder. The aim of the work is to identify the best processing conditions for the manufacturing of near-net-shape, chemically-homogeneous and fine-grained Ti-6Al-7Nb components. Specifically, a comparison of the microstructural features, final relative density and hardness obtained when processing the Ti-6Al-7Nb titanium alloy by different powder metallurgy techniques, precisely cold uniaxial pressing and sintering, uniaxial conventional hot-pressing and uniaxial inductive hot-pressing, is carried out.

2. Experimental Procedure

2.1 Starting materials

The starting materials include an elemental titanium powder and a niobium:aluminium:titanium (Nb:Al:Ti) master alloy, which were purchased from GfE Gesellschaft für Elektrometallurgie mbH, as well as an elemental aluminium powder (Sulzer Metco Ltd). Some characteristics of the starting powders provided by the suppliers are shown in Table 1.

Table 1. Characteristics of the starting powders (supplier specifications).

Material	Production method	Composition [wt.%]	Particle morphology	Maximum size [µm]
Elemental Ti	Hydride-dehydride (HDH)	> 99.7	Irregular	< 75
Nb:Al:Ti	Metallothermic reduction + vacuum induction melting and casting	60:35:5	Granules	< 800
Elemental Al	Gas atomisation	> 99	Spherical	< 150

From Table 1 it can be seen that the elemental titanium powder used was produced by means of the HDH process. Its employment prevents the problems connected with the presence of chlorides in sponge titanium powders already described in the introduction. Elemental aluminium was used in order to obtained the right ratio of alloying elements (i.e. aluminium/niobium) because the purchased Nb:Al:Ti master alloy does not have the desired ratio.
From the data reported in Table 1, it can also be noticed that the maximum particle size of the purchased Nb:Al:Ti master alloy is significantly greater with respect to the other powders. To prevent segregation during the handling of the powder, to uniform the size of the powders and to favour the diffusion of the alloying elements during sintering, it was decided to reduce the particle size of the purchased Nb:Al:Ti master alloy by using a Fritsch Pulverisette high-energy ball mill. The details of the process and parameters used are available in a previous publication [7].

2.2 Production and characterisation of the Ti-6Al-7Nb powder

The Ti-6Al-7Nb alloy was produced by mixing elemental titanium and the milled Nb:Al:Ti (47:40:13) master alloy for 30 minutes in a Turbula mixer. Figure 1 which shows a scheme of the powder production route employed.

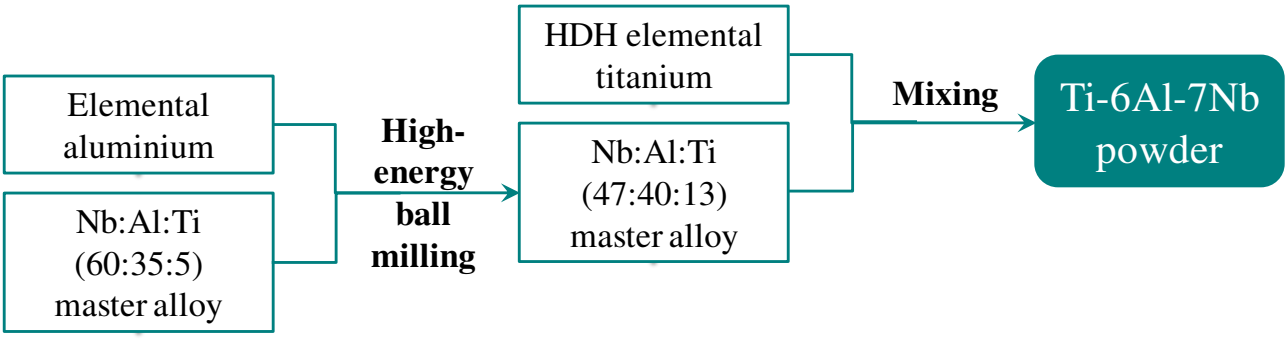

Figure 1. Scheme of the production route employed to fabricate the Ti-6Al-7Nb powder.

The particle size distribution and, therefore, the maximum particle size D_{max} of both the milled master alloy and the fabricated Ti-6Al-7Nb alloy powders were measured by means of a laser beam Mastersizer 2000 particle size analyser. Oxygen and nitrogen contents were measured by inert gas fusion method using a LECO TC500 equipment on the base of the ASTM E1409 standard for oxygen and ASTM E1937 standard for nitrogen.

Carbon content was determined by combustion technique using a LECO CS200 equipment following the ASTM E1941 standard. The morphology of the Ti-6Al-7Nb powder was checked using a Philips XL–30 SEM in backscattered mode. The density of the powder was measured by helium picnometry using a Micromeritics Accupyc 1330 analyser. Important processing properties for industries, such as apparent density and the flow rate, were determined on the base of the MPIF 04, MPIF 28 and MPIF 03 standards, respectively, using Hall and/or Carney apparatus. Other important industrial properties, such as the compressibility (MPIF 45) and the green strength (MPIF 15) were measured varying the consolidation pressure in the 300-700 MPa range using a conventional hydraulic uniaxial press to shape the powder.

2.3 Consolidation of the powder

The prepared Ti-6Al-7Nb powder was consolidated by means of three powder shaping techniques: cold uniaxial pressing and sintering (P&S), uniaxial conventional hot-pressing (CHP) and uniaxial inductive hot-pressing (IHP).

For the P&S route, green specimens were cold uniaxially pressed at 700 MPa using a floating die and zinc stearate as lubricant for the walls of the die. The samples were subsequently sintered in a high vacuum (10^{-5} mbar) tubular furnace using a heating and cooling rate of 5°C/min. In a preliminary study, the sintering temperature was ranged between 900ºC and 1400ºC, step of 100ºC, and the dwell time was set to 2 hours. In a second stage, the green samples were sintered in a narrow sintering temperature window (1250-1350ºC) considering the effect of the sintering time, namely 2 hours and 4 hours. It is worth mentioning that a dwell step of 30 minutes at 300ºC was added to the sintering thermal cycle to favour the elimination of the wax used as process control agent (PCA) during the milling of the Nb:Al:Ti master alloy.

Concerning the uniaxial CHP method, the Ti-6Al-7Nb powder was poured into a graphite mould lined out with a low reactive graphite foil. In order to prevent the direct interaction of the powder with the graphite punches at high temperature, graphite foils coated with a high temperature ceramic boron nitride (BN) spray were placed in between them. The BN coating was also useful to facilitate mould release. Before proceeding with the CHP experiment, the powder was cold uniaxially pressed at approximately 18 MPa using a manual press. The temperatures employed to sinter the powder were 900ºC, 1100ºC and 1300ºC, using a heating rate of 10ºC/min and a minimum vacuum level of 10^{-1} mbar. By means of thermocouples placed directly in contact with the graphite mould, a deviation of ± 5ºC of the processing temperature was guaranteed. The uniaxial pressure applied was set to 30 MPa and cooling of the samples was performed by switching off the heating elements (furnace cooling) with the simultaneous removing of the pressure. The dwell time at maximum temperature was 1 hour for 900ºC and 1100ºC and 30 minutes for 1300ºC. The time selected for each temperature corresponds to an effective dwell time of 30 minutes at the maximum processing temperature due to the inertia of the system which induces a delay between the programmed and real temperature.

For the uniaxial IHP experiments, a homemade press composed of a stainless steel vacuum chamber, a servo-hydraulic test machine (LF 70S) capable of dynamic loads up to 70 kN with a frequency up to 70 Hz and a self-adjusting inductive heating system (output power of 30 kW and frequency range between 20-150 kHz) was used. The control of the temperature was done by means of a pyrometer which guarantees a precision of ± 5ºC. The sintering temperatures studied were 1100ºC and 1300ºC using a heating rate of 50ºC/min.

The applied pressure was 50 MPa, the dwell time at maximum temperature was set to 15 min and a minimum vacuum level of 10^{-3} mbar was guaranteed. The cooling of the samples was carried out by cutting off the powder supply and simultaneously removing the applied pressure.
Figure 2 displays a comparison of the thermal cycles used for each one of the powder metallurgy processing technique employed in this study.

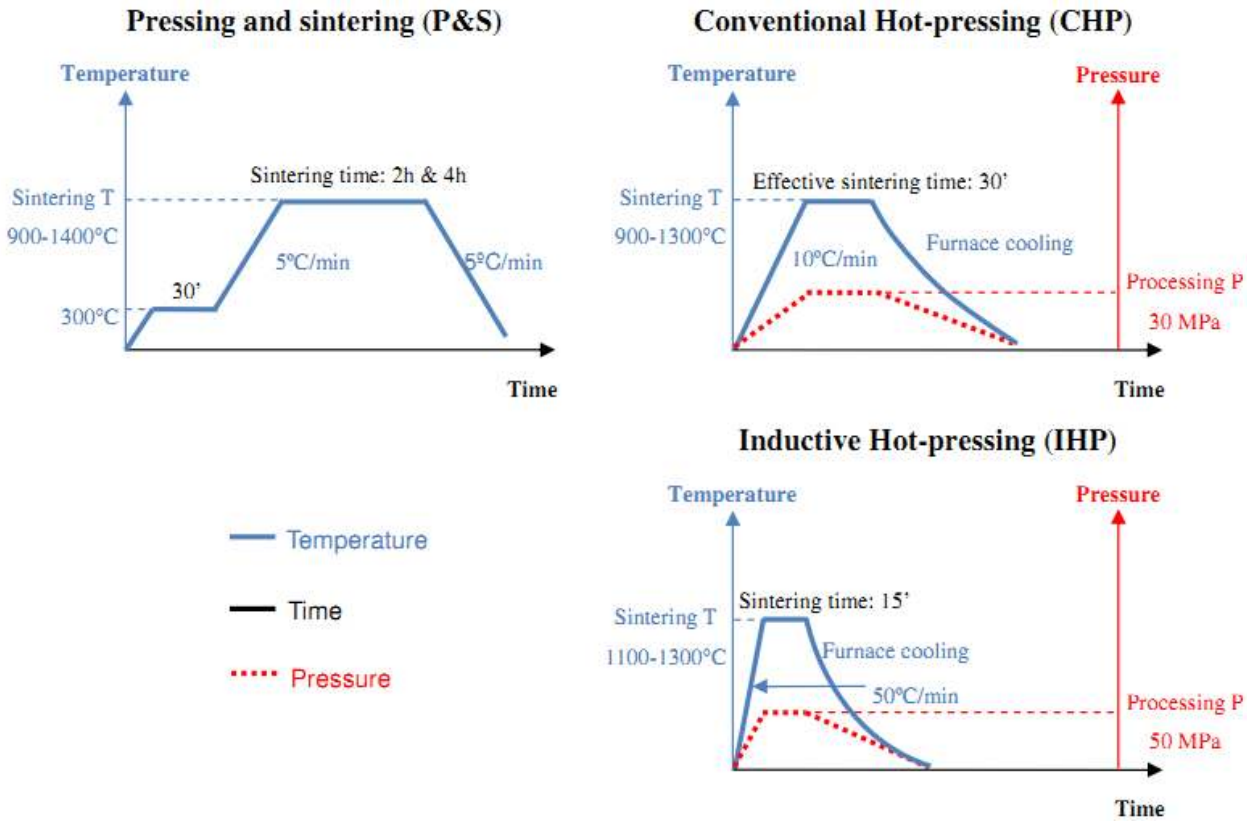

Figure 2. Schemes of the processing cycles used to consolidate the Ti-6Al-7Nb powder.

From the sketches reported in Figure 2, it can be said that the total processing time decreases from 12-18 hours of the P&S route to approximately 6 hours for the CHP method and to less than 1 hour for the IHP technique. This clearly depends on the application of the uniaxial pressure and, especially, on the heating system that is the possibility to use much greater heating rates and, in turns, to reduce the production costs.
Before their characterization, the samples produced by both CHP and IHP were sandblasted to clean the surfaces that had been in contact with the processing tools. For microstructural analysis, the classical metallographic preparation route was followed: grinding with SiC papers, polishing with alumina solution and final polishing using silica gel. The microconstituents were revealed by means of chemical etching using Kroll's reagent (3 ml HF + 6 ml HNO_3 + 100 ml H_2O). An Olympus GX71 optical microscope was used for the analysis of the microstructure of the sintered samples. The density of the samples produced by the different powder metallurgy routes previously described was obtained by means of water displacement measurements. The total porosity left was calculated as a difference with respect to the theoretical value of the wrought Ti-6Al-7Nb alloy, which is 4.52 g/cm^3 [8]. Concerning the mechanical properties, the variation in the hardness with sintering temperature was measured by means of a Wilson Wolpert Universal Hardness DIGI-TESTOR 930 tester performing HV30 measurements.

3. Results and Discussion

3.1 Characterisation of the powder

As explained in the experimental procedure, the purchased Nb:Al:Ti (60:35:5) master alloy was milled in order to reduce its particle size and to adjust the composition. Table 2 shows the results of the particle size distribution for samples of the milled Nb:Al:Ti (47:40:13) master alloy that were collected every 15 minutes during 90 minutes.

Table 2. Particle size distribution of the milled Nb:Al:Ti (47:40:13) master alloy as a function of the milling time.

Milling time [min]	D_{10} [µm]	D_{50} [µm]	D_{90} [µm]
15	5.83	24.55	108.97
30	**4.94**	**17.84**	**54.34**
45	2.47	20.08	98.15
60	2.23	17.90	79.76
75	4.36	12.59	45.18
90	1.99	12.31	49.89

From the data reported in Table 2, it can be seen that the maximum particle size of the master alloy is drastically reduced already after 15 minutes of milling. Moreover, it can also be noticed that the particle size further decreases at 30 minutes but then increases at 45 minutes to decrease again for longer milling time. This swinging behaviour is due to the typical processes that characterise the milling of ductile powders since during high-energy milling the powder particles are repeatedly flattened, cold welded, fractured and rewelded [9].
From Table 2, the shortest milling to obtain a particle size similar to that of the HDH elemental titanium powder is 30 minutes because it permits to obtain a particle size lower than 55 µm. Consequently, this was considered as the optimum milling time and the powder produced was used to fabricate the Ti-6Al-7Nb alloy.
The results of the chemical analysis carried out on the Nb:Al:Ti (47:40:13) master alloy milled during 30 minutes are shown in Table 3.

Table 3. Chemical analysis of the Nb:Al:Ti (47:40:13) master alloy milled during 30 minutes.

Element	Content [wt.%]
Oxygen	1.130
Nitrogen	0.0879
Carbon	0.634

From table 3, it can be seen that oxygen content is greater than 1 wt.% even though the Nb:Al:Ti master alloy was milled under inert gas atmosphere (argon) to prevent or at least minimise oxidation during milling whereas nitrogen content is lower than 0.01 weight percentage. The relatively high carbon content of the milled Nb:Al:Ti master alloy is due to the wax used as PCA in order to prevent adhesion of the powder to the vessel or to the grinding media.

Particle size distribution and chemical analysis were also carried out on the Ti-6Al-7Nb powder obtained by mixing elemental titanium and the milled Nb:Al:Ti (47:40:13) master alloy. The results are reported in Table 4 together with the values of density, apparent density and flow rate.

Table 4. Particle size distribution, chemical analysis and industrial processing properties of the produced Ti-6Al-7Nb powder.

Property		**Ti-6Al-7Nb**
Particle size analysis	**D_{max} [µm]**	< 90
	D_{10} [µm]	17.40
	D_{50} [µm]	40.39
	D_{90} [µm]	81.94
Chemical analysis	**O [wt %]**	0.393
	N [wt %]	0.0173
	C [wt %]	0.0706
ρ_{He} [g/cm^3]		4.4748
ρ_{app} Hall [g/cm^3]		–
Flow rate [s/50g]		–
ρ_{app} Carney [g/cm^3]		2.04 ± 0.011

From the particle size distribution data obtained for the produced Ti-6Al-7Nb powder, it can be seen that the D_{90} parameter is 81.94 µm and, thus, the powder can be classified as a 170 mesh powder (D < 90 µm). Oxygen content is slightly lower than 0.4 wt.% whereas nitrogen content is about 0.02 wt. %. Carbon content is relatively high (0.08 wt.%) but the value reported in Table 4 should not be considered as the carbon content dissolved into the titanium matrix since it is significantly increased by the presence of the wax used as PCA during milling of the Nb:Al:Ti master alloy. The presence of the wax also influences, in particular lowers, the value of the density of the powder obtained by helium picnometry with respect to the nominal value of the wrought Ti-6Al-7Nb (4.52 g/cm^3). Measurements of the apparent density and flow rate by means of the Hall apparatus could not be performed due to the morphology of the powder. The apparent density was therefore measured by Carney apparatus with the help of a wire to agitate the powder to promote its flow as specified in the MPIF 28 standard and it gives as a result 2.04 g/cm^3.

The morphology of the Ti-6Al-7Nb powder was analysed by SEM and a representative example is reported in Figure 3 where it can be seen that the three powders used to produce the Ti-6Al-7Nb alloy powder, which could be clearly distinguished using the BSE mode due to the different atomic number of the elements, have very similar particle size and morphology. By means of the morphology analysis different features could be highlighted: 1) it is confirmed that the HDH elemental titanium powder is irregular in shape and, therefore, suitable for the conventional P&S powder metallurgy route; 2) the shape of the elemental aluminium powder is not perfectly spherical but slightly deformed due to the fact that the powder was milled altogether with the Nb:Al:Ti master alloy; 3) the particle size of the Nb:Al:Ti master alloy was effectively reduced, its maximum particle is approximately 50 µm in agreement with the particle size distribution analysis (Table 2) and its morphology is irregular.

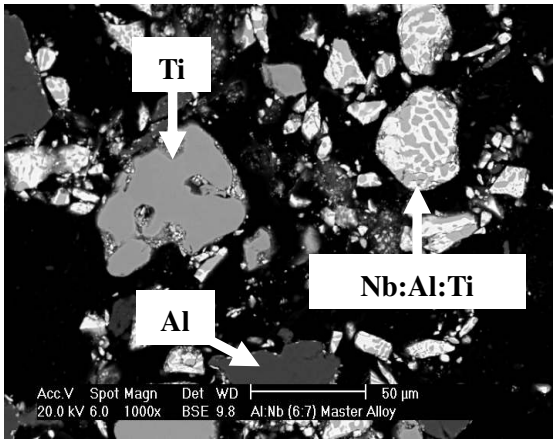

Figure 3. SEM micrograph (BSE mode) showing the morphology of the Ti-6Al-7Nb powder.

The results of the compressibility test and of the green strength of the Ti-6Al-7Nb samples are shown in Figure 4.

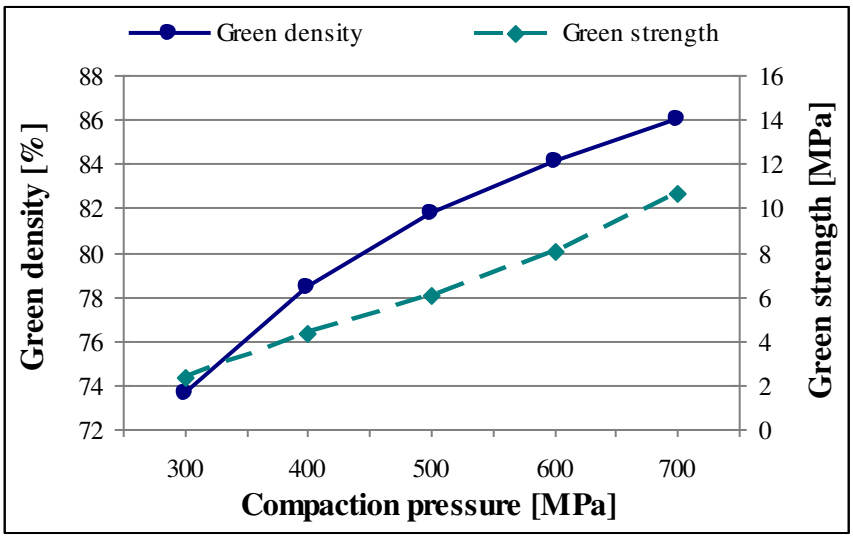

Figure 4. Compressibility and green strength of the Ti-6Al-7Nb alloy.

As it can be seen in Figure 4, the compressibility of the Ti-6Al-7Nb powder increases with the increment of the compaction pressure, reaching a maximum value of 86%. The green strength of the cold uniaxially pressed samples has a similar trend. Therefore, the higher the compaction pressure, the higher the green strength where the maximum value is approximately 11 MPa. The values of the relative density and green strength shown in Figure 4 are comparable to those obtained by the authors in previous works about titanium alloys produced using HDH powders [10].

A good compressibility is a very important factor for powder to be used for the P&S route since the higher the green density, the lower the shrinkage of the part during sintering which, in turns, results in a lower dimensional change of the final shape of a component. Consequently, based on the characterisation carried out, the compaction pressure of 700 MPa was selected for the production of the samples to be sintered.

3.2 Microstructure of sintered materials

The microstructural evolution with the processing temperature for cold uniaxially P&S samples is presented in Figure 5.

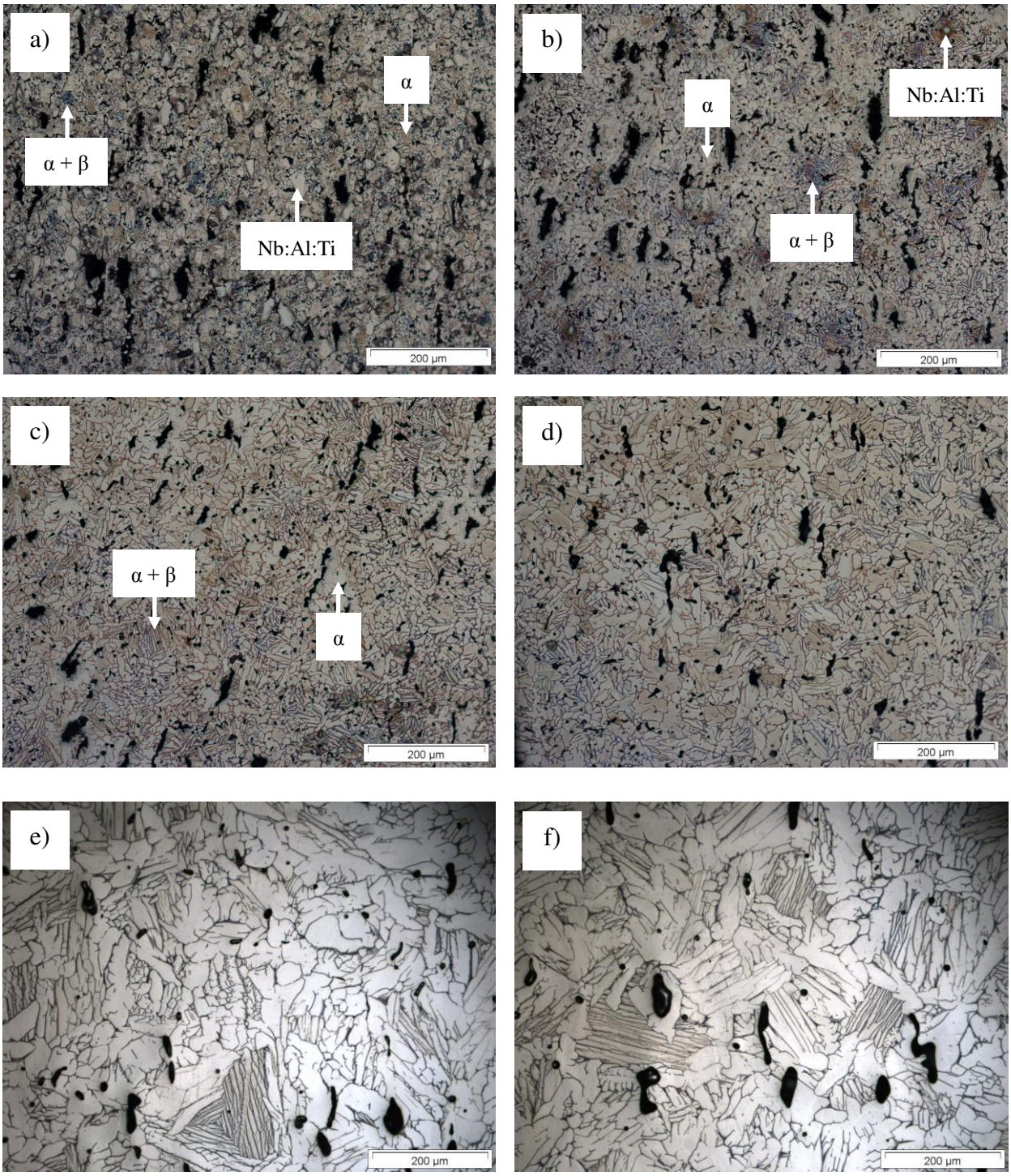

Figure 5. Optical micrographs of cold uniaxially P&S Ti-6Al-7Nb samples sintered for 2 hours: a) 900ºC, b) 1000ºC, c) 1100ºC, d) 1200ºC and e) 1300ºC, and sintered for 4 hours f) 1300ºC.

From Figure 5 a), at a processing temperature of 900ºC, the sintering of the material has already initiated because interparticle necking between the powder particles are clearly seen. Nevertheless, many interparticle boundaries of the former powder particles are still present.

The poor densification induced by the low sintering temperature leads to a pore structure mainly composed by angular and interconnected pores. From Figure 5 a), it can also be noticed that at the sintering temperature of 900ºC, the diffusion of the alloying elements toward the titanium matrix has just begun. Consequently, the microstructure is mainly constituted by elemental alpha titanium grains even if some fine and localised two-phase α + β islands are present in the microstructure. These islands are likely to be found near the former Nb:Al:Ti master alloy particles where locally the amount of niobium already diffused in the titanium matrix is sufficiently high to stabilise the beta phase, because the maximum solubility of niobium in α-Ti is 2.2 ± 0.5 at.% [11]. Another interesting feature of the P&S samples sintered at 900ºC is the presence of porosity inside and near the former Nb:Al:Ti master alloy particles. This kind of porosity is most probably due to the differences in terms of self-diffusion and interdiffusion coefficients between elemental titanium and the alloying elements as well as among the alloying elements. Actually the diffusion rate of aluminium in titanium is two orders of magnitude higher than that of niobium [12] and this results in the formation of Kirkendall porosity [13-15]. The microstructure of the P&S specimens sintered at 1000ºC looks like that of those processed at 900ºC but some important differences can be highlighted: the pore structure is somewhat less interconnected even though the pores are still mostly irregular, and the distribution of the alloying elements is more homogeneous but not terminated yet. As a consequence of the greater diffusion of the alloying elements, bigger and more uniformly distributed α + β regions are found together with alpha titanium grains. Using a sintering temperature of 1100ºC for the processing of the P&S Ti-6Al-7Nb samples leads to a much more homogeneous microstructure composed by alpha grains with an even distribution of α + β lamellae throughout the whole microstructure. Although the distribution of the alloying elements seems uniform and the diffusion processes completed, EDS analysis reveals that a minimum sintering temperature has to be used to guarantee that the alloying elements complete dissolve inside the titanium matrix [16]. When using a sintering temperature of 1100ºC the amount of residual porosity is still quite important as it can be clearly seen in Figure 5 c). The employment of a sintering temperature higher than 1100ºC permits to obtain the typical laminar microstructure of the α + β titanium alloys composed by alpha grains and α + β lamellae (Figure 5 d-e). With the increment of the sintering temperature the pores get more spherical and tend to move towards the grain boundaries and coalesce at three-point boundaries. Therefore, the pore structure is composed of far less, isolated and slightly larger pores. Finally, the increment of the processing temperature leads also to coarser microconstituents where the alpha grains grow at the expense of the α + β lamellae which become longer and thinner. The effect of using a longer processing time (4 hours) can be seen in Figure 5 f) where the specimens are characterised by coarser microconstituents (α grains and α + β lamellae) and some few relatively large pores.

The microstructural evolution with the processing temperature CHP Ti-6Al-7Nb specimens is shown in Figure 6 where it can be seen that the microstructure of the CHP Ti-6Al-7Nb samples processed at 900ºC (Figure 6 a) is composed by alpha titanium grains and undissolved Nb:Al:Ti master alloy particles albeit fine two-phase α + β islands are uniformly distributed throughout the whole microstructure. This result indicates that the selected temperature/time combination is not appropriate to guarantee the complete dissolution of the Nb:Al:Ti master alloy particles and the diffusion of the alloying elements because most of the former Nb:Al:Ti master alloy particles are still visible even though their particle size is generally smaller. The pore structure is composed by irregular and elongated pores and most of them are located near the Nb:Al:Ti particles indicating that this porosity is a consequence of the Kirkendall effect.

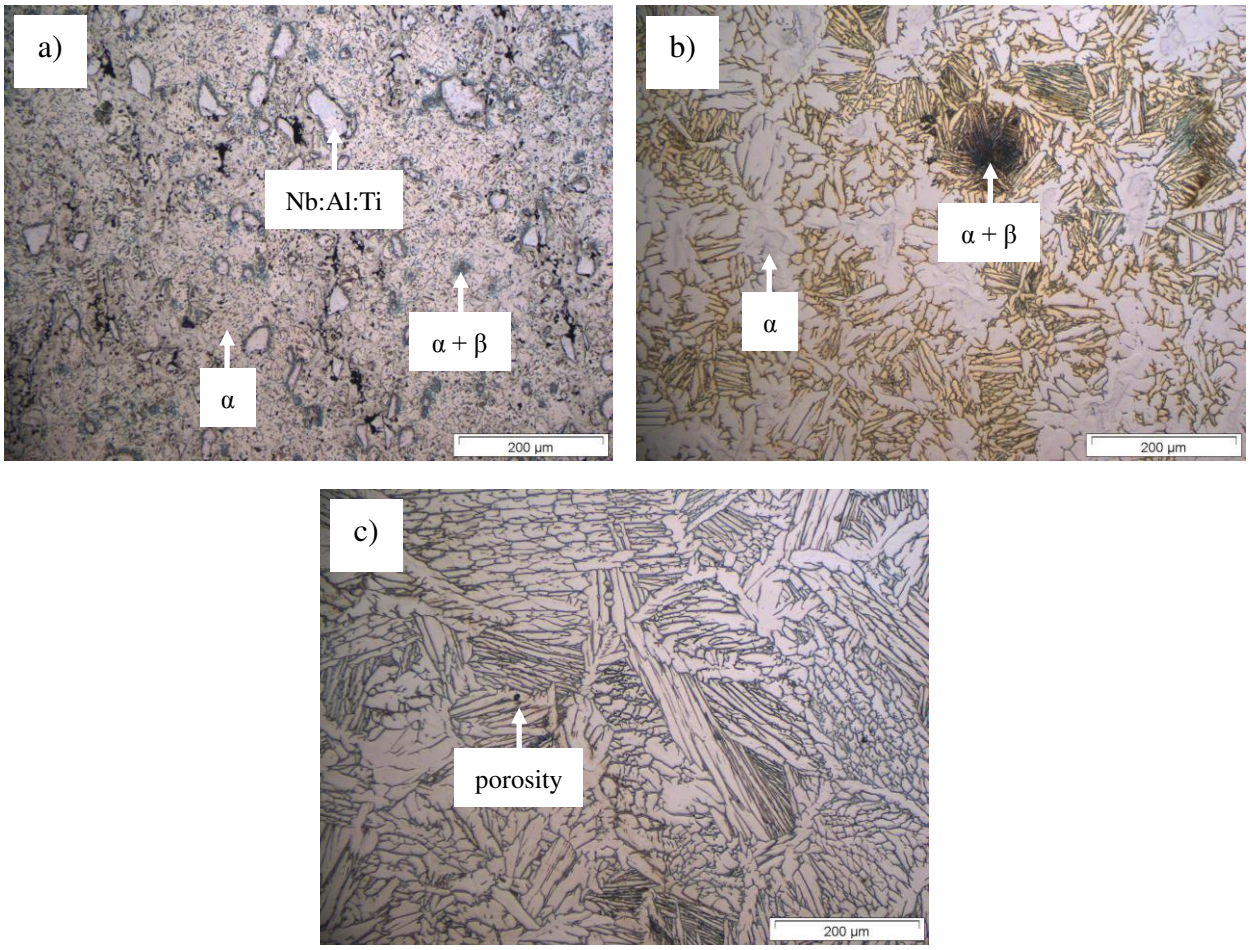

Figure 6. Optical micrographs of CHP Ti-6Al-7Nb samples: a) 900ºC, b) 1100ºC and c) 1300ºC.

When the Ti-6Al-7Nb powder is uniaxially hot-pressed at 1100ºC (Figure 6 b), the material is characterised by a heterogeneous microstructure of alpha grains plus large α + β lamellae and a distribution of very fine and localised two-phase α + β islands. It can be said that the distribution of the alloying elements in the titanium matrix is not homogenous because of the presence of the small two-phase islands and of the uneven distribution of the α + β lamellae in the microstructure. Once again, the two-phase α + β islands are likely to be placed in the proximity of the former Nb:Al:Ti master alloy particles where the local amount of niobium dissolved in titanium is very high. An important difference in comparison to the samples produced using the processing temperature of 900ºC is the lower amount of residual porosity that can be seen in the cross-section of the samples even though some small pores can still be found throughout the microstructure, especially near the two-phase α + β islands (Kirkendall porosity). In this case the residual porosity is much smaller in size and completely isolated. From Figure 6 c), it can be seen that the employment of a processing temperature of 1300ºC leads to a homogeneous microstructure composed by alpha grains and a uniform distribution of α + β lamellae confirming the complete diffusion of the alloying elements in the titanium matrix. The microstructure shown in Figure 6 c) is the typical laminar microstructure usually obtained by the slow cooling through the two-phase α + β region of the α + β titanium alloys from above the beta transus. Very few, small and isolated pores can be seen in the microstructure positioned in the grain boundaries suggesting that practically fully dense samples are produced.
The micrographs of the Ti-6Al-7Nb specimens fabricated by consolidation of the powder by IHP are displayed in Figure 7.

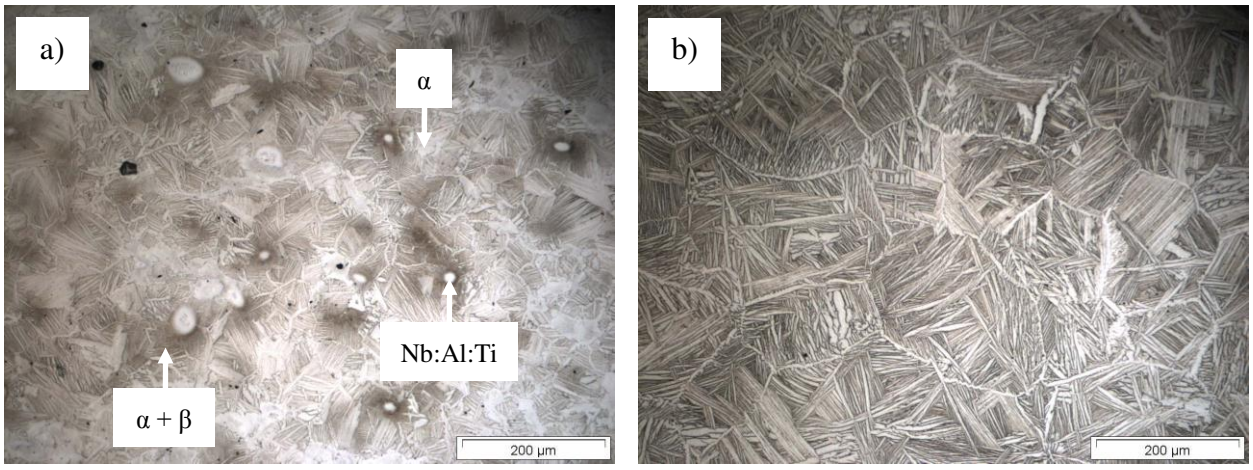

Figure 7. Optical micrographs of IHP Ti-6Al-7Nb samples: a) 1100ºC and b) 1300ºC.

The processing of the Ti-6Al-7Nb at 1100ºC by means of IHP (Figure 7 a) leads to a heterogeneous microstructure composed by grains and α + β acicular grains. The presence of these α + β acicular grains is justified by the fast cooling rate typical of the field-assisted sintering techniques (FAST) where the densification of the powder is assisted by an external current [17, 18]. Moreover, due to the very short processing time, the full chemical homogenization of the alloying elements is not reached and partially undissolved former Nb:Al:Ti master alloy particles can still be identified in the microstructure. Predominantly spherical and isolated pores can also be seen in the microstructure of the samples processed at 1100ºC. When the sintering temperature is set to 1300ºC, the microstructure obtained resembles that of the samples processed at 1100ºC because is still composed by alpha grains and fine α + β acicular grains. Actually, from Figure 7 b), it can be seen that the alpha phase is most probably located at the former interparticle boundaries and the needle-like α + β phase is found within these alpha phase boundaries. As checked by EDS analysis, the diffusion of the alloying elements is completed and their distribution homogeneous, hence no original Nb:Al:Ti master alloy particles are found. Furthermore, fully dense samples are fabricated because almost no porosity is present.

From the comparison of the results of the microstructural analysis of the Ti-6Al-7Nb samples produced by P&S, CHP and IHP, it seems that independently of the consolidation technique a sintering temperature higher than 1100ºC must be used to guarantee the homogeneous distribution of the alloying elements. Clearly the time at temperature and, in turns, the total processing time is reduced by the application of a uniaxial load during the sintering of the powder. A more drastic reduction of the processing time is then achieved by the simultaneous application of the uniaxial load with an external current. The sintering of the material by simultaneously applying temperature and pressure normally reduces also the total amount of residual porosity for a specific processing temperature. Moreover, the pore structure is more commonly composed by spherical and isolated pores rather than irregular and interconnected. No significant differences in terms of microconstituents can be highlighted between the P&S and CHP samples but the microconstituents (alpha grains and α + β lamellae) are generally coarser in the P&S samples due to the longer time at maximum temperature that the material experiences when using the P&S route. Instead of the α + β lamellae typical of the slow cooled Ti-6Al-7Nb alloy, the IHP samples are characterised by the classic basketweave Widmanstätten microstructure of fast cooled α + β titanium alloy.

As previously explained, this microstructure is a direct consequence of the fast cooling intrinsic of the FAST methods. Apart from the presence of acicular α + β grains, the microconstituents of the IHP samples are generally much finer due to the the short time at temperature that can be selected.

3.3 Relative density of sintered materials

The variation of the density of the Ti-6Al-7Nb samples and the trend of residual porosity are presented in Figure 8 a) and Figure 8 b), respectively.

a)

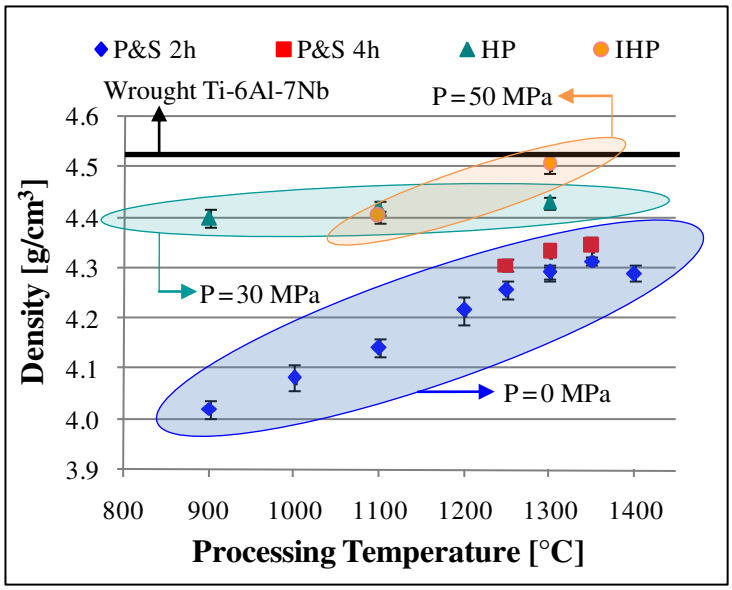

b)

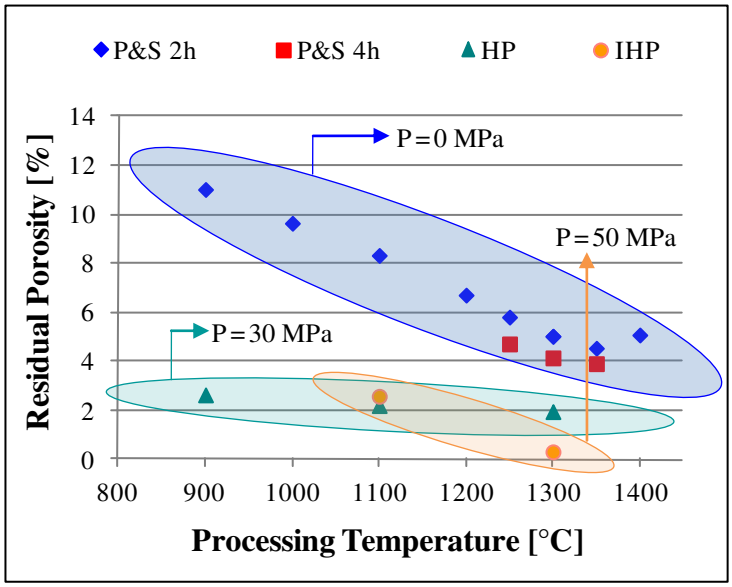

Figure 8. Density (a) and residual porosity (b) of sintered Ti-6Al-7Nb samples as a function of the processing temperature.

Considering the data of the cold uniaxially P&S Ti-6Al-7Nb samples shown in Figure 8 a), it can be seen that the density of the specimens increases with the increment of the processing temperature and the trend can be represented by an asymptotic curves.

The trend of the density indicates that the densification of the material during sintering takes place mostly in the sintering temperature range from 900ºC to 1200ºC. This result is in agreement with the microstructural evolution described on the base of the micrographs of P&S samples (Figure 5). Actually from 900ºC to 1200ºC most of the thermal energy supplied to the system is invested for the formation of necking between the particle, elimination of interparticle boundaries and diffusion of the alloying elements. On the other side, from the processing temperature of 1200ºC, the pore structure is already composed of spherical and isolated pores (second stage of sintering) and a further increment of the sintering temperature induces the coarsening of both the pores and the microconstituents. In this case the density ranges between approximately 4.02 g/cm^3 and 4.31 g/cm^3 which correspond to relative density values in between 89% and 95% of the nominal density or, in turns, is equivalent to a total residual porosity which decreases from 11% to 5% (Figure 8 b). These residual porosity values match well with the amount of porosity which can be seen in the micrographs of the P&S samples (Figure 5). The density values shown in Figure 8, especially for the highest processing temperatures, are comparable to those obtained by other authors which considered the blending elemental approach to produce titanium alloys using elemental titanium powders (sponge or HDH) blended with elemental powders or master alloys [19-22].

From Figure 8, it can also be noticed that the employment of a longer sintering time for the P&S samples leads to somewhat higher density and, as consequence, slightly lower residual porosity. However, the increment in density or the reduction in porosity is in the order of 1% which does not justify the higher processing cost of doubling the sintering time from 2 hours to 4 hours.

Concerning the density values of the Ti-6Al-7Nb specimens obtained by CHP, it can be seen that there is a little increment with the processing temperature but it is not very important because increases from 4.40 g/cm^3 to 4.43 g/cm^3. The relative density values calculated from the data shown in Figure 8 range between 97.4% and 98.0% and, thus, a total percentage of residual porosity which decreases from 2.6% to 2.0% (Figure 8 b). These amounts of residual porosity are higher than the ones that could be expected on the base of the microstructural analysis (Figure 6) where, with the exception of the powder sintered at 900ºC, very few, small and isolated pores were found. Though the increment of the hot-pressing temperature does not influence significantly the final density of the material, it has been demonstrated by means of the micrographs shown in Figure 6 that it is necessary to employ a relatively high processing temperature in order to guarantee the complete diffusion of the alloying elements and to obtain microstructures with homogeneous distribution of the microconstituents. The behaviour of the master alloy addition Ti-6Al-7Nb powder (i.e density values and microstructural evolution) during its processing by CHP is similar to that of the Ti-6Al-7Nb powder fabricated using elemental powders [23] but the formation of the Al_3Ti intermetallic, which normally takes place when mixing elemental powders [24], is prevented.

From the data of the density of the IHP Ti-6Al-7Nb samples, a significant increment of the final density is measured when increasing the sintering temperature from 1100ºC to 1300ºC. In particular, the density increases from 4.40 g/cm^3 to 4.51 g/cm^3 (97.4% and 99.7%, respectively) and the residual porosity decreases from 2.6% to 0.3%. In the case of IHP, the residual porosity values seem to be in agreement with the microstructural analysis shown in Figure 7. No terms of comparison could be found in the literature for the processing of the Ti-6Al-7Nb alloy by means of FAST processes but, generally, fully dense materials are produced with these methods [17].

When comparing the density value obtained for the different powder metallurgy techniques used to consolidate the Ti-6Al-7Nb powder, it can be seen that actually the application of a uniaxial pressure during the sintering step is beneficial.

There is a quite important advantage in applying the pressure at low sintering temperature (especially at 900ºC) since the final density is notably higher. This effect is somewhat mitigated at intermediated processing temperatures (1100-1200ºC) even though the difference in terms of relative density is still 6%. The gap between the density values of pressureless and hot-pressed materials narrows at high sintering temperature (1300-1400ºC) but the difference becomes greater if a higher uniaxial pressure is used. Even so, similar high sintering temperatures have to be set to produce materials with homogeneous distribution of the alloying elements and uniform microstructures.

3.4 Hardness of sintered materials

The values of the hardness measurements carried out on the cross-section of the Ti-6Al-7Nb samples are represented as a function of the processing temperature and relative density in Figure 9.

a)

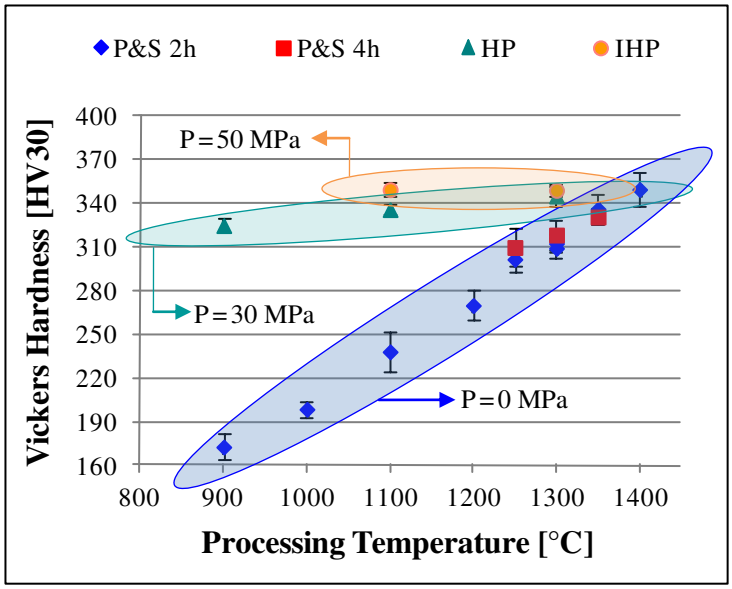

b)

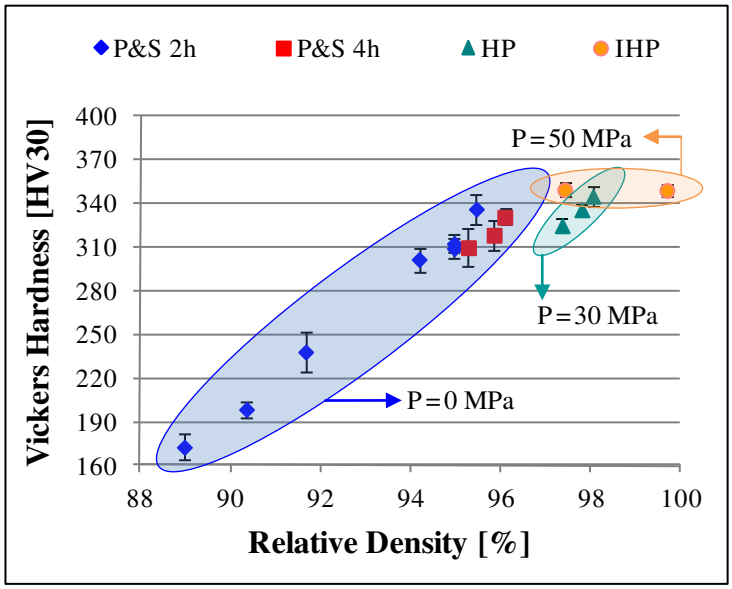

Figure 9. Variation of the Vickers hardness (HV30) as a function of the processing temperature (a) and as a function of the relative density of the samples (b).

From Figure 9 a), it can be seen that the hardness of the P&S specimens increases continuously with the processing temperature. This is the common behaviour of powder metallurgy materials since the higher the sintering temperature, the lower the residual porosity (Figure 8) and, consequently, the higher the hardness. The absolute values range between 170 HV30 for a processing temperature of 900ºC to 350 HV30 when sintering the material at 1400ºC.

The nominal hardness value of the wrought Ti-6Al-7Nb is in between 290 HV, as specified for the production of biomedical devices (IMI 367 alloy) [25], and 350 HV as reported by the authors that developed the alloy at the early nineteen eighties [26]. The low hardness value of the samples sintered in the 900-1100ºC sintering temperature range is mainly a consequence of the high percentage of residual porosity but could also be affected by the poor diffusion and heterogeneous distribution of the alloying elements into the titanium matrix (Figure 5). Actually, the values shown in Figure 9 are comparable to those of commercially pure (CP) titanium, which range in between 162 HV for CP2 and 253 HV for CP4 [8]. At the sintering temperature of 1200ºC, where the microstructure is fully developed and homogeneous, the P&S material equals the hardness of the IMI 367 alloy even though the presence of almost 7% of residual porosity. At higher temperature the hardness of P&S samples increases reaching 350 HV30 with still something like 5% of total porosity. This behaviour is due to the higher interstitials contents, especially oxygen, that the material considered in this study has (Table 4) with respect to the nominal value of the wrought alloy (0.20 wt.% for oxygen and 0.05 wt.% for nitrogen) [8]. Different studies demonstrated that the higher the amount of interstitials (oxygen, nitrogen, hydrogen and carbon) dissolved in titanium, the harder the material [27-29]. Considering each specific processing temperature, the P&S Ti-6Al-7Nb samples sintered for longer time (4 hours) are basically characterised by the same hardness of their counterpart sintered during 2 hours. Knowing that the density is higher (Figure 8) and expecting a higher amount of interstitials for longer processing times, the hardness of the specimens sintered for 4 hours is lowered by the grain growth.

About the variation of the hardness of the CHP Ti-6Al-7Nb samples, it can be seen in Figure 9 a) that there is a small increment in hardness, from 325 HV30 to 345 HV30 when increasing the processing temperature from 900ºC to 1300ºC. As shown in Figure 8, the density of the CHP specimens is quite constant with the increment of the sintering temperature and the residual porosity is approximately 2%. Because the effect of the density on the hardness can be excluded, the gentle increment of the hardness is due to the homogenisation of the distribution of the alloying elements and of the microconstituents. In particular, the high Vickers hardness of the samples hot-pressed at 900ºC is due to the balance between the low hardness of elemental titanium, which constitutes the matrix, and the high hardness of the former Nb:Al:Ti master alloy particles embedded in it. These Nb:Al:Ti master alloy particles are most probably composed by intermetallics such as Nb_3Al, Nb_2Al and Al_3Nb whose hardness is in the range of 800 HV [30, 31]. At a processing temperature of 1100ºC, the dissolution of the particle is almost completed but the microstructure is composed by a much higher percentage of fine two-phase $\alpha + \beta$ islands and, in turns, a lower amount of alpha titanium, justifying that the hardness is maintained constant. When processed at 1300ºC there is not influence from the intermetallics but the material is characterised by the typical microstructure of $\alpha + \beta$ and achieves the hardness of the wrought alloy. Finally, it can be said that the gentle increment of the hardness with the processing temperature is favoured by the expected increment of the interstitials dissolved and disfavoured by the grain growth that the material undergoes. Once again, the higher content of interstitials, especially oxygen (Table 4), is the responsible for the higher hardness in comparison to the IMI367 alloy.

From Figure 9 a), it can be seen that the hardness of the IHP specimens remains constant at 350 HV30 with the increment of the processing temperature. This behaviour is the balance of the factors previously described for P&S and CHP samples: decrement of residual porosity, presence of Nb:Al:Ti master alloy particles embedded into the Ti matrix, homogenisation of the distribution of the alloying elements and of the microconstituents and increment of interstitials content.
The comparison of the hardness values obtained when processing the Ti-6Al-7Nb alloy by means of different powder metallurgy techniques is better carried out considering the relative density values of the samples (Figure 9 b). Knowing that there is not significant oxygen pick-up when processing the Ti-6Al-7Nb powder the three powder metallurgy techniques employed, it can be stated that the relative density is the most important factor affecting the final hardness of the material studied because CHP and IHP samples processed at 900º or 1100ºC are characterised by a non-homogeneous distribution of the alloying elements but still have much higher hardness in comparison to P&S specimens sintered at the same temperature. Therefore, the application of a uniaxial pressure during the sintering of the Ti-6Al-7Nb alloy seems to be beneficial, in terms of hardness achievement, at relatively low processing temperature. This effect fades with the increment of the sintering time because the residual porosity of P&S samples in significantly reduced and comparable hardness values are obtained when a pore structure composed by isolated pores is present in the material (94%) [32]. On the base of this finding, it can also be seen that the application of a higher uniaxial pressure and the employment of an external current do not improve significantly the final hardness of the alloy because the relative density values are similar.

4. Conclusions

From the comparison of the microstructure and properties of the Ti-6Al-7Nb alloy produced considering the master alloy addition approach and processed by different powder metallurgy techniques, namely cold uniaxial pressing and sintering, uniaxial conventional hot-pressing and uniaxial inductive hot-pressing, it can be concluded that:

- Near net-shape, chemically-homogeneous and fine-grained titanium-based components with properties similar to those of the wrought materials can be produced by means of powder metallurgy;
- Independently of the powder metallurgy technique employed, a sintering temperature higher than 1100ºC must be used to guarantee the homogeneous distribution of the alloying elements;
- The sintering time is not as influencing the properties studied as the sintering temperature;
- The simultaneous application of a uniaxial pressure and temperature for the consolidation of the powder as well as the employment of an external current are beneficial in terms of final density and to significantly reduce the total processing time.

Acknowledgments

The authors are thankful for the financial support from the Spanish Ministry of Education through the R&D MAT2009-14448-C02-02 and MAT2009-14547-C02-02 Projects and from Comunidad de Madrid through the ESTRUMAT (S-2009/MAT–1585) project. Moreover, the authors would like to thank Dr. Erik Neubauer from RHP-Technology GmbH and Co. KG for giving the possibility to carry out the hot-pressing experiments.

References

[1] K. Faller, F.S. Froes, The Use of Titanium in Family Automobiles: Current Trends, JOM, 53 (2001) 27-28.

[2] M. Long, H.J. Rack, Titanium Alloys in Total Joint Replacement - A Materials Science Perspective, Biomaterials, 19 (1998) 1621-1639.

[3] M. Niinomi, Recent metallic materials for biomedical applications, Metallurgical and Materials Transactions A, 33 (2002) 477-486.

[4] M. Semlitsch, F. Staub, W. H., Titanium-aluminium-niobium Alloy Development for Biocompatible, High Strength Surgical Implants, Biomedizinische Technik/Biomedical Engineering, 30 (1985) 334–339.

[5] V.A. Druz, V.S. Moxson, R. Chernenkoff, W.F. Jandeska Jnr, J. Lynn, Blending an Elemental Approach to Volume Titanium Manufacture, Metal Powder Report, 61 (2006) 16-21.

[6] M.J. Donachie, Titanium. A Technical Guide, 2nd Edition ed., ASM International, Ohio, USA, 2000.

[7] L. Bolzoni, E.M. Ruiz-Navas, E. Neubauer, E. Gordo, Inductive Hot-pressing of Titanium and Titanium Alloy Powders, Materials Chemistry and Physics, 131 (2012) 672-679.

[8] R. Boyer, G. Welsch, E.W. Collings, Materials Properties Handbook: Titanium Alloys, in: A. International (Ed.), Ohio, USA, 1998.

[9] C. Suryanarayana, Mechanical Alloying and Milling, Progress in Materials Science, 46 (2001) 1-184.

[10] L. Bolzoni, P.G. Esteban, E.M. Ruiz-Navas, E. Gordo, Influence of Powder Characteristics on Sintering Behaviour and Properties of PM Ti Alloys Produced from Prealloyed Powder and Master Alloy, Powder Metallurgy, 54 (2011) 543-550.

[11] J.L. Murray, Phase Diagrams of Binary Titanium Alloys, 1st ed., ASM International, 1987.

[12] N.L. Peterson, Diffusion in Rfractory metals, WADD Technical Report, (1960) 123-149.

[13] E.O. Kirkendall, Transaction AIME, 147 (1942) 104.

[14] A.D. Smigelskas, E.O. kirkendall, Transaction AIME, 171 (1947) 130.

[15] F. Seitz, On the Porosity Observed in the Kirkendall Effect, Acta Metallurgica, 3 (1953) 355–369.

[16] L. Bolzoni, E.M. Ruiz-Navas, T. Weissgaerber, B. Kieback, E. Gordo, Mechanical Behaviour of Pressed and Sintered CP Ti and Ti-6Al-7Nb Alloy Obtained from Master Alloy Addition Powder, Journal of the Mechanical Behavior of Biomedical Materials, Accepted Manuscript (2012).

[17] R. Orrù, R. Licheri, A.M. Locci, A. Cincotti, G. Cao, Consolidation/Synthesis of Materials by Electric Current Activated/Assisted Sintering, Materials Science and Engineering R: Reports, 63 (2009) 127-287.

[18] Z.A. Munir, U. Anselmi-Tamburini, M. Ohyanagi, The Effect of Electric Field and Pressure on the Synthesis and Consolidation of Materials: A Review of the Spark Plasma Sintering Method, Journal of Material Science, 41 (2006) 763-777.

[19] S. Abkowitz, D. Rowell, Superior Fatigue Properties for Blended Elemental P/M Ti-6Al-4V, Journal of Metals, (1986) 36-39.

[20] F.H. Froes, O.M. Ivasishin, V.S. Moxson, D.G. Savvakin, K.A. Bondareva, A.M. Demidik, Cost-effective Synthesis of Ti–6Al–4V Alloy Components via the Blended Elemental P/M Approach, in: W. TMS, PA (Ed.) Symposium on TMS Symposium on High Performance Metallic Materials for Cost Sensitive Applications, Seattle, WA, 2002.

[21] J.E. Smugeresky, D.B. Dawson, New Titanium Alloys for Blended Elemental Powder Processing, Powder Technology, 30 (1981) 87-94.
[22] D. Eylon, P.R. Smith, S.W. Schwenker, F.H. Froes, Status of Titanium Powder Metallurgy, in: Webster/Young (Ed.) Industrial Applications of Titanium and Zirconium: 3rd Conference, ASTM International, 1984, pp. 48-65.
[23] V.A.R. Henriques, C.E. Bellinati, C.R.M. da Silva, Production of Titanium Alloys for Medical Implants by Powder Metallurgy, Key Engineering Materials Advanced Powder Technology II (2001) 443-448.
[24] A. Böhm, B. Kieback, Investigation of Swelling Behaviour of Ti-Al Elemental Powder Mixtures during Reaction Sintering, Zeitschrift für Metallkunde, 89 (1998) 90-95.
[25] D. Henry, Materials and Coatings for Medical Devices: Cardiovascular, ASM International, Ohio, USA, 2009.
[26] M. Semlitsch, H. Weber, R. Steger, Fifteen Years Experience with Ti-6AI-7Nb Alloy for Joint Replacements, in: P.A. Blenkinsop, Evans, W. J., Flower, H. M. (Ed.) Titanium '95: Science and Technology, Birmingham - UK, 1995, pp. 1742-1759.
[27] R.I. Jaffee, I.E. Campbell, The Effect of Oxygen, Nitrogen and Hydrogen on Iodide Refined Titanium, Transactions of the American Institute of Mining and Metallurgical Engineers, 185 (1949) 646-654.
[28] R.I. Jaffee, H.R. Ogden, D.J. Maykuth, Alloys of Titanium with Carbon, Oxygen and Nitrogen, Transactions of the American Institute of Mining and Metallurgical Engineers, 188 (1950) 1261-1266.
[29] W.L. Finlay, J.A. Snyder, Effects of Three Interstitial Solutes (Nitrogen, Oxygen and Carbon) on the Mechanical Properties of High-purity Alpha Titanium, Journal of Metals 188 (1950) 277-286.
[30] L. Murugesh, K.T. Venkateswara Rao, R.O. Ritchie, Powder Processing of Ductile-phase-toughened Nb-Nb3Al in situ Composites, Materials Science and Engineering A, 189 (1994) 201-208.
[31] C. Triveño Rios, P. Ferrandini, R. Caram, Fracture Toughess of the Eutectic Alloy Al3NB-Nb2Al, Materials Letters, 57 (2003) 3949-3953.
[32] R.M. German, Powder Metallurgy Science, 2nd Edition ed., MPIF - Metal Powder Industries Federation, Princeton, USA, 1994.